Secondary Structure and Backbone Resonance Assignments of the Periplasmic Cyclophilin Type Peptidyl-Prolyl Isomerase from *Escherichia coli*†

Robert T. Clubb, Venkataraman Thanabal, Jasna Fejzo, Stephen B. Ferguson, Lynne Zydowsky, C. Hunter Baker, Christopher T. Walsh, and Gerhard Wagner*

Department of Biological Chemistry and Molecular Pharmacology, Harvard Medical School, 240 Longwood Avenue, Boston, Massachusetts 02115

Received December 17, 1992; Revised Manuscript Received April 13, 1993

ABSTRACT: Proton, carbon-13, and nitrogen-15 sequence-specific backbone assignments have been obtained for the periplasmic cyclophilin type *cis–trans* peptidyl-prolyl isomerase from *Escherichia coli* (167 residues, M_r = 18 244). Assignments were obtained using both ^1H, ^{13}C, and ^{15}N triple-resonance and ^1H and ^{15}N double-resonance three-dimensional (3D) NMR spectroscopy at pH 6.2, 25 °C. Complete or partial residue-specific assignments have been obtained for 165 of the 167 residues. The secondary structure has been characterized using long- and medium-range NOEs. The protein consists of an eight-stranded anti-parallel β-sheet and two helices. The overall topology of *E. coli* cyclophilin is similar to that of human T-cell cyclophilin. Sequence alignment with human T-cell cyclophilin based on secondary structure homology implicates several residues in *E. coli* cyclophilin that may be crucial for binding the peptide substrate AC-A-A-P-A-AMC and the immunosuppressive drug cyclosporin A.

The periplasmic cyclophilin type *cis–trans* peptidyl-prolyl isomerase from *Escherichia coli* (eCyP)[1] is a member of a superfamily of enzymes that includes two structural branches: the cyclophilins (CyP) and the FK-binding proteins (FKBP). These enzymes catalyze the *cis–trans* isomerization of Xaa–Pro amide bonds in small peptides and in proteins in the later stages of folding (Fischer et al., 1989; Takahashi et al., 1989). There is a large range of potential physiological substrates for these enzymes. The best described case is the folding of rhodopsin by an eye tissue specific cyclophilin homolog known as nina A (Ondek et al., 1992). The mechanism of catalytic Xaa–Pro bond isomerization is likely to involve the induction of strain and the distortion of a nonplanar amide transition state in a hydrophobic active site microenvironment. Both cyclophilin and FKBP are of interest for separate pharmacological reasons. Cyclophilin and FKBP are targets for the blockade of graft rejection and T-cell activation by the immunosuppressant drugs cyclosporin A (CsA) (Handshumacher et al., 1984; Harding et al., 1986) and FK506 (Harding et al., 1989; Siekierka et al., 1989), respectively. Immunosuppression is thought to occur in the T-cell when the complex of CyP/CsA or FKBP/FK506 binds to and inhibits the calcium- and calmodulin-dependent protein serine phosphatase, calcineurin (Liu et al., 1991b).

Two cyclophilin isomerases, one cytoplasmic and one periplasmic, have been cloned, sequenced, and purified from *E. coli* (Liu & Walsh, 1990; Hayano et al., 1991). These two proteins are approximately 50% identical in amino acid sequence (Hayano et al., 1991) and exhibit significantly reduced affinities for the drug CsA, relative to hCyP (hCyP, IC_{50} = 6 nM; periplasmic eCyP, IC_{50} = 3000 nM) (Handschumacher et al., 1984; Harding et al., 1986; Liu et al., 1990). Interestingly, a single point mutation at position 112 in periplasmic eCyP (F112W) results in a 25-fold increase in affinity for CsA. In addition the periplasmic F112W eCyP/CsA complex binds and inhibits calcineurin (F. A. Etzkorn, L. A. Stolz, Y. Shi, and C. T. Walsh, manuscript in preparation).

Several structural studies have been conducted on human cyclophilin. Crystal structures have been reported for unliganded isoform A of human T-cell CyP (hCyPA) (Ke et al., 1991) and an hCyPA/tetrapeptide complex (Kallen et al., 1991; Kallen & Walkinshaw, 1992). NMR investigations have revealed the secondary structure of human cyclophilin (Neri et al., 1991; Wüthrich et al., 1991), and hCyPA/CsA interactions have been identified (Neri et al., 1991; Spitzfaden et al., 1992; Fesik et al., 1992). The conformation of CsA bound to hCyPA has also been determined (Fesik et al., 1991; Weber et al., 1991).

We have undertaken structural studies of wild-type eCyP utilizing NMR spectroscopy. A high-resolution structure of eCyP should help to elucidate the mechanism of *cis–trans* peptidyl-prolyl isomerization and explain the decreased affinity of *E. coli* cyclophilin for CsA relative to hCyP. Furthermore, a comparison of the structures of eCyP and hCyP will aid in determining common structural determinants essential for calcineurin inhibition. As a first step in this process, we have used double- and triple-resonance NMR spectroscopy to sequence-specifically assign the backbone resonances of the protein. Resonance assignments reveal that eCyP consists of an eight-stranded anti-parallel β-sheet and at least two stretches of residues that adopt a helical conformation. Secondary structure alignments with human cyclophilin implicate several residues in eCyP that should play key roles

† This research was supported by NIH Grant GM 47467. Partial support was obtained from Grants GM 38608 to G.W. and GM 20011 to C.W. and by NIH NSRA Grant 14252 to S.B.F.

* Address correspondence to this author.

[1] Abbreviations: AC, *N*-acetyl; AMC, amidomethylcoumarin; CsA, cyclosporin A; CyP, *Escherichia coli* cyclophilin type peptidyl-prolyl isomerase; DQF-COSY, two-dimensional double quantum filtered correlation spectroscopy; HMQC, heteronuclear multiple quantum coherence; HSQC, heteronuclear single quantum coherence; INEPT, insensitive nuclei enhancement by polarization transfer; NMR, nuclear magnetic resonance; NOE, nuclear Overhauser enhancement; NOESY, two-dimensional nuclear Overhauser enhancement spectroscopy; PPIase, *cis–trans* peptidyl-prolyl isomerase; SCUBA, stimulated cross peaks under bleached α; TOCSY, two-dimensional total correlation spectroscopy; TSP, 3-(trimethylsilyl)propionate.

0006-2960/93/0432-6391$04.00/0

in binding peptide/protein substrates and the immunosuppressant drug CsA.

MATERIALS AND METHODS

Protein Expression and Purification. Development of the expression vector, pJLEC-2B, for the truncated form of the periplasmic eCyP (residues 23–190) has been reported (Liu & Walsh, 1990). Uniformly ^{15}N and $^{13}C/^{15}N$ isotopically labeled proteins were obtained from 1-L cultures of pJLEC-2B/XA90 in enriched celtone media (microalgae extracts from Martek Corp., celtone-N, 98% ^{15}N, and celtone-CN, 98% ^{13}C and ^{15}N) containing 100 μg/mL ampicillin. Cultures were incubated at 37 °C until A_{595} reached 1.0. Isopropyl β-D-thiogalactopyranoside (IPTG) was added to a final concentration of 2 mM, and the incubation was continued for 6 h. Purification involved modifications of the previously reported protocol (Liu & Walsh, 1990). Approximately 7 g of cells was harvested, suspended in 42 mL of 20 mM Tris·HCl buffer (pH 8.0), and cracked by a French press. After centrifugation, 2.5 mL of 2% protamine sulfate was added slowly. The supernatant was dialyzed overnight [2 × 3 L of 20 mM Tris·HCl buffer (pH 8.0)] and passed through a DEAE–Sepharose CL-6B column (1 × 15 cm). The 167-residue protein was collected as the flow-through fractions and concentrated to the appropriate millimolar concentrations for NMR analysis. A similar protocol was used for preparing three residue-specific ^{15}N-labeled proteins using the pJLEC-2B/XA90 prototropic strain. The only modification involved the use of amino acid enriched minimal medium (2 L). The growth medium (Muchmore et al., 1989) includes 18 unlabeled amino acids and the single ^{15}N-labeled amino acid. The ^{15}N-labeled lysine and phenylalanine amino acids were obtained from Isotec Inc., and labeled valine was obtained from Cambridge Isotope Laboratory.

NMR Sample Preparation. NMR samples were typically 0.2-2 mM eCyP in 400 μL of 50 mM phosphate buffer. The pH (uncorrected for isotope effects) was adjusted to 6.2. Spectra collected with H_2O as the solvent contained 5% (v/v) ^2H_2O to establish a lock signal. When ^2H_2O was used as the solvent, the protein was lyophilized and resuspended in ^2H_2O twice. In between lyophilizations, the protein was incubated in ^2H_2O for approximately 1 day at 35 °C; this process resulted in nearly complete exchange of amide protons for deuterons.

NMR Spectroscopy. All spectra were recorded at 25 °C on 500- and 600-MHz Bruker AMX spectrometers. Unless otherwise stated, reported sweep widths were at 600 MHz. NMR data were processed on both Sparc SLC (Sun Microsystems) and Iris (Silicon Graphics, Inc.) workstations using FELIX (Hare Research, Inc.). Experiments were collected in the quadrature mode. Prior to Fourier transformation, the data were multiplied with appropriately matched sine bell squared window functions in both t_1 and t_2. Proton chemical shifts are referenced to TSP. Carbon-13 chemical shifts are referenced to external dioxane (67.8 ppm). Nitrogen-15 chemical shifts are referenced to $NH_4{}^{15}NO_2$ in ^2H_2O (25 °C, 376.25 ppm).

Homonuclear NMR Spectroscopy. Homonuclear NOESY (Jeener et al., 1979; Kumar et al., 1980), TOCSY (Braunschweiler & Ernst, 1983), and DQF-COSY (Piantini et al., 1984; Shaka & Freeman, 1983; Rance et al., 1984) spectra were acquired on an unlabeled eCyP sample (1 mM) in both H_2O and ^2H_2O. A sweep width of 9615 Hz was used in both proton dimensions. Low-power continuous wave saturation was employed during the relaxation delay (1.3 s) to suppress the H_2O signal. The SCUBA technique (Brown et al., 1988) was utilized in the NOESY and TOCSY experiments recorded in H_2O to recover saturated proton resonances under the water line. All experiments employed time-proportional phase incrementation (TPPI) for sign discrimination along ω_1 (Marion & Wüthrich, 1983).

Double-Resonance 3D NMR Spectroscopy. 3D NOESY-HMQC and TOCSY-HMQC spectra were acquired as previously described (Fesik & Zuiderweg, 1988; Marion et al., 1989a; Zuiderweg & Fesik, 1989). Spectra were recorded on a 1 mM uniformly ^{15}N-enriched sample of eCyP in H_2O. SCUBA delays were employed to recover saturated α-proton resonances. The relaxation delay was 1.3 s. Sweep widths of 8333, 2016, and 9615 Hz were used in the ω_1, ω_2, and ω_3 dimensions, respectively. TPPI was used in the t_1 and t_2 dimensions to achieve frequency sign discrimination. NOESY-HMQC and TOCSY-HMQC spectra were acquired with 256, 32, and 1024 real t_1, t_2, and t_3 values, respectively. The NOESY-HMQC experiment was recorded with a mixing time of 100 ms and a total of 32 scans per transient. The TOCSY-HMQC experiment used a 35-ms DIPSY-2 mixing scheme (Shaka et al., 1988) with 16 scans per transient. Acquisition times of 120 and 60 h were used for the NOESY-HMQC and TOCSY-HMQC experiments, respectively. Both 3D matrices were zero-filled, resulting in a final frequency domain data set of 512 × 128 × 512 points in ω_1, ω_2, and ω_3, respectively. The final digital resolutions in ω_1, ω_2, and ω_3 were 16.3, 15.8, and 4.7 Hz per point, respectively. The HCCH-COSY experiment (Kay et al., 1990b; Bax et al., 1990a) was recorded on a 700 μM sample of eCyP. Approximately 70% of this sample was uniformly (>95%) enriched with nitrogen-15 and carbon-13, while 30% of the sample was unintentionally enriched with nitrogen-15 only. The source of the unenriched protein is unknown. A total of 128, 32, and 512 complex points were utilized in t_1, t_2, and t_3, respectively. Sweep widths of 7143 (^1H), 3205 (^{13}C), and 9615 (^1H) Hz were used in ω_1, ω_2, and ω_3, respectively. Sign discrimination in the indirect dimensions was obtained by the States–TPPI method (Marion et al., 1989b). The total time for acquisition was ca. 90 h (16 scans per increment).

Two-dimensional ^1H–^{13}C and ^1H–^{15}N heteronuclear single quantum coherence (HSQC) spectra (Morris & Freeman, 1979; Bodenhausen & Ruben, 1980) were recorded with sweep widths of 2016 and 7143 Hz for the ^{15}N and ^{13}C frequency domains, respectively. No presaturation of the H_2O resonance was used in the ^1H–^{15}N HSQC experiments; instead, a single purge pulse was employed to destory the H_2O signal (Messerli et al., 1989). The ^1H–^{13}C HSQC spectrum was acquired in ^2H_2O.

Triple-Resonance 3D NMR Spectroscopy. All experiments were performed on a 1.5 mM sample of uniformly double-labeled eCyP in H_2O (pH 6.2, 25 °C) unless otherwise stated. The experimental details of the constant-time HNCA and HN(CO)CA experiments have been described elsewhere (Kay et al., 1990a; Bax & Ikura, 1991; Grzesiek & Bax, 1992). A spin lock was used in both experiments to eliminate the H_2O resonance instead of continuous presaturation (Messerli et al., 1989). In the CT-HNCA experiment, 62, 128, and 512 real points were acquired in t_1, t_2, and t_3, respectively. In the CT-HN(CO)CA experiment, 64, 120, and 512 real points were acquired in t_1, t_2, and t_3, respectively. Both experiments used TPPI to obtain sign discrimination in t_1 and t_2. In each experiment, sweep widths of 2016, 6757, and 9615 Hz were used in ω_1, ω_2, and ω_3, respectively. CT-HNCA and CT-HN(CO)CA experiments each required ~70 h of acquisition time. The HN(CA)HA experiment (Clubb et al., 1992; Kay

et al., 1992) was run with constant-time nitrogen-15 evolution (t_1) with 58, 72, and 1024 real points in t_1, t_2, and t_3, respectively. Sweep widths of 2016, 2874, and 9515 Hz were used in ω_1, ω_2, and ω_3, respectively. The HN(CA)HA experiment was acquired for ca. 84 h. The constant-time HCA(CO)N experiment was performed on a 1.5 mM sample of ^{13}C–^{15}N eCyP in ^2H_2O (Kay et al., 1990a; Powers et al., 1992). A total of 50, 58, and 512 real points were used in t_1, t_2, and t_3, respectively. Sweep widths 1748, 3571, and 3521 Hz (at 500 MHz) were used in ω_1, ω_2, ω_3, respectively. The experiment was acquired for 96 h (96 transients per increment).

The HNCO and HCACO spectra were acquired as described by Kay et al. (1990a). Both experiments were performed on a 700 μM sample of eCyP uniformly enriched with nitrogen-15 and 70% enriched with carbon-13. The HNCO experiment was conducted in H_2O with 32, 128, and 512 real points in t_1, t_2, and t_3, respectively. Low-power continuous wave saturation was employed during the relaxation delay (1.3 s) to suppress the H_2O signal. Sweep widths of 2016, 2232, and 9615 Hz were used in ω_1, ω_2, and ω_3, respectively. The HCACO experiment was performed in ^2H_2O with 48, 96, and 512 points in t_1, t_2, and t_3, respectively. Sweep widths of 4237, 2232, and 9615 Hz were used in ω_1, ω_2, and ω_3, respectively. HNCO and HCACO experiments were each acquired for ~105 h.

RESULTS

Assignment of backbone ^1H, ^{13}C, and ^{15}N resonances was accomplished by use of both triple- and double-resonance NMR techniques. Three-dimensional ^1H–^{15}N-edited experiments were performed on a uniformly ^{15}N-enriched sample of eCyP. Three-dimensional triple-resonance spectra were recorded on a doubly labeled ^{13}C–^{15}N sample of the protein. Interpretation of these spectra allowed groups of spin systems to be linked both by conformation-dependent nuclear Overhauser enhancements and by conformation-independent scalar correlations. These groups were then sequence-specifically placed by identifying the amino acid type of several members of each stretch. Amino acid type identification was accomplished by analysis of ^1H (DQF-COSY and TOCSY) and ^{13}C (HCCH-COSY) scalar experiments and/or by selective nitrogen-15 enrichment according to amino acid type. Assignments facilitated the identification of medium- and long-range nuclear Overhauser enhancements, allowing the secondary structural elements of eCyP to be elucidated.

Assignments

Double-Resonance Experiments. The strategy used to analyze the three-dimensional ^1H–^{15}N-edited spectra has been described previously (Fesik & Zuiderweg, 1988; Marion et al., 1989a; Zuiderweg & Fesik, 1989; Driscoll et al., 1990; Clubb et al., 1991; Fairbrother et al., 1991; Stockman et al., 1992). In brief, it involves the identification of intraresidue correlations in 2D ^1H NMR spectra (DQF-COSY, TOCSY) and in the 3D ^1H–^{15}N TOCSY-HMQC spectrum (Marion et al., 1989a). Conformation-dependent nuclear Overhauser enhancements (NOEs) in the 3D ^1H–^{15}N NOESY-HMQC spectrum (Fesik & Zuiderweg, 1988; Zuiderweg & Fesik, 1989; Marion et al., 1989a) are then used to sequentially link adjacent spin systems. Strong d_{NN} connectivities are used to sequentially link adjacent residues involved in turns or helices. Residues participating in extended strand conformations are sequentially linked via $d_{\alpha N}$ connectivities.

Sequence-specific assignments utilizing single- and double-resonance techniques alone were difficult due to the low sensitivity of experiments relying on ^1H–^1H scalar couplings (DQF-COSY, TOCSY, etc.). Reduced sensitivity is attributed to the large proton line widths exhibited by eCyP (^1H > 30 Hz), which hinder scalar coupling dependent coherence transfer. As a consequence, only 94 of 155 potential ^{15}N–$^1H^N$–$^1H^\alpha$ correlations (167–11 prolines–N-terminus) were obtained from the TOCSY-HMQC spectrum with very few residues exhibiting ^{15}N–$^1H^N$–$^1H^\beta$ correlations. Longer mixing times for this experiment did not yield a significantly increase in the number of correlations. The lack of intraresidue scalar information made it difficult to distinguish intra- and interresidue NOEs in the HMQC-NOESY spectrum. In general, linkage of adjacent spin systems was quite facile; difficulties arose, however, in determining the directionality of most peptide pairs.

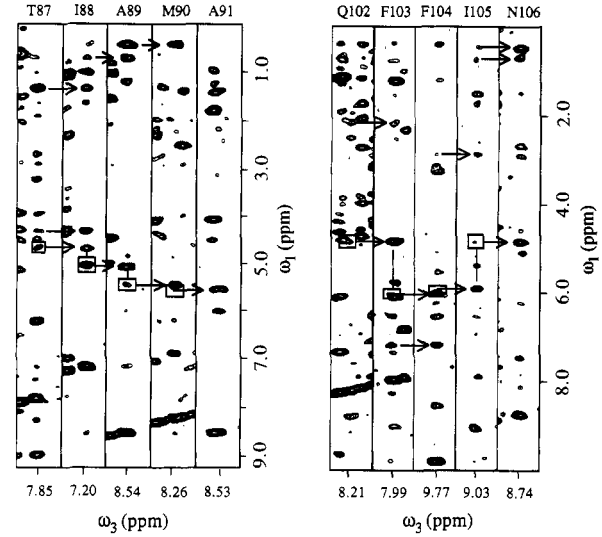

FIGURE 1: Panels corresponding to $\omega_1 \times \omega_3$ slices of the 3D NOESY-HMQC spectrum of ^{15}N-labeled eCyP. Slices are taken at the ω_2 axis position corresponding to the backbone amide nitrogen frequency of residues 87–91 (A, left) and residues 102–106 (B, right). Residue numbers and the corresponding $^1H^N(\omega_3)$ chemical shift are indicated at the top and bottom of each slice, respectively. For clarity, each slice contains only 0.3 ppm of the ω_3 axis. Intraresidue $^1H^N$–$^1H^\alpha$ cross peaks are shown boxed, with arrows indicating $d_{\alpha N}$ connectivities.

In those cases where there was sufficient intraresidue information, double-resonance methods proved sufficient to obtain sequence-specific assignments. The assignments of Thr87 to Ala91 and Glu102 to Asn106 are demonstrated in Figure 1A,B, respectively. Panels correspond to sections of the 3D NOESY-HMQC spectrum taken at the ω_2 amide nitrogen chemical shifts of the residues indicated at the top of the figure. Intraresidue H^N to H^α cross peak positions are enclosed in boxes. Close inspection reveals that often this intraresidue cross peak does not appear in the NOESY-HMQC spectrum (e.g., M90, F103, F104); its position, however, was confirmed by analysis of the TOCSY-HMQC and HN(CA)-HA spectra (data not shown). Each panel contains NOEs arising from the amide proton of the indicated residue. For example, the panel corresponding to Ile88 exhibits strong NOEs to the preceding residue, Thr87. In particular, an intense $d_{\alpha N}$ connectivity links these residues. Residues Thr87 to Ala91 and Glu102 to Asn106 form part of strands 5 and 6 of the β-sheet, respectively (see Figure 4). On the basis of secondary structure alignments with human cyclophilin residues, Glu102 and Phe104 in eCyP are likely to be important in binding the tetrapeptide AC-A-A-P-A-AMC (Kallen et al., 1991; Kallen & Walkinshaw, 1992), and Phe104 may be essential for binding CsA (Fesik et al., 1992). A more detailed

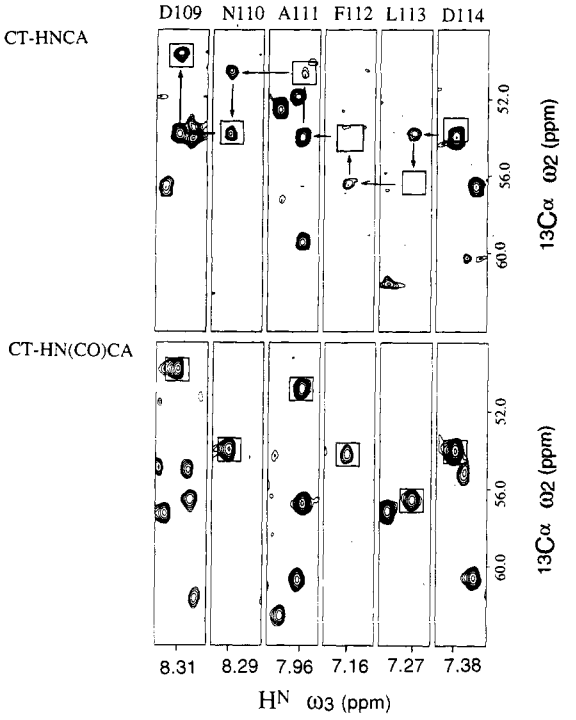

FIGURE 2: HNCA and HN(CO)CA spectra of ^{13}C–^{15}N-labeled eCyP. The top set of panels are $\omega_2 \times \omega_3$ slices of the HNCA spectrum. Slices contain the resonances of residues 109–114. Each panel is taken at a fixed nitrogen-15 frequency corresponding to the amide nitrogen chemical shift (ω_2) of the indicated residue. The lower set of panels contains the corresponding $\omega_2 \times \omega_3$ slices of the HN(CO)CA spectrum of the same set of residues. Sequential $^1H^N_{(i)}$–$^{15}N_{(i)}$ to $^{13}C^{\alpha}_{(i-1)}$ cross peaks are enclosed in boxes in both spectra.

secondary structure alignment with hCyP is presented in the Discussion section.

As mentioned above, assignment of most side-chain spin systems proved to be difficult due to the paucity of intraresidue information present in ^1H scalar spectra. This obstacle was overcome by analysis of the HCCH-COSY spectrum (Kay et al., 1990b; Bax et al., 1990a) of a ^{13}C–^{15}N-labeled sample of eCyP and by preparation of three samples of eCyP selectively enriched with nitrogen-15. The HCCH-COSY spectrum in favorable cases allowed the $^1H^{\alpha}$–$^{13}C^{\alpha}$ correlations of each residue to be linked with their corresponding side-chain nuclei. The side-chain identity of each residue could then be deduced by either its spin topology and/or the chemical shift of its $^{13}C^{\beta}$ nuclei (distinct $^{13}C^{\beta}$ and $^1H^{\beta}$ chemical shifts are exhibited by some side-chain types, i.e., serine and threonine residues often have downfield-shifted $^{13}C^{\beta}$ and $^1H^{\beta}$ nuclei). In addition to the analysis of HCCH-COSY spectrum, three eCyP samples were prepared, each enriched with nitrogen-15 only in valine, lysine, or phenylalanine residues. A ^1H–^{15}N HSQC spectrum of each of these samples was then acquired and the ^1H–^{15}N cross peak was identified as belonging to a particular amino acid type (McIntosh et al., 1990). In the above example (Figure 1B), nitrogen-15 enrichment of all phenylalanine amino acids was crucial in obtaining the sequence-specific assignment of residues 102–106. Phenylalanine-specific enrichment identified those cross peaks associated with panels 103 and 104 as arising from amide protons of phenylalanine residues. The phenylalanine pair (Phe103–Phe104) is unique in the amino acid sequence of eCyP.

In order to expedite the assignment process and to resolve proton chemical shift degeneracy in backbone and side-chain nuclei, NMR studies were conducted on a doubly labeled sample (carbon-13 and nitrogen-15) of eCyP. This allowed the application of triple-resonance NMR spectroscopy to assign the majority of backbone nuclei in eCyP (Ikura et al., 1990; Kay et al., 1990a).

Triple-Resonance Experiments. Backbone assignment procedures for doubly labeled proteins are well documented (Ikura et al., 1990). The assignment strategy used for eCyP employed six triple-resonance experiments. These were performed on two doubly labeled samples of eCyP. CT-HNCA (Kay et al., 1990a; Grzesiek & Bax, 1992). CT-HN(CO)CA (Bax & Ikura, 1991; Grzesiek & Bax, 1992), CT-HCA(CO)N (Kay et al., 1990a; Powers et al., 1991), and CT-HN(CA)HA (Clubb et al., 1992; Kay et al., 1992) spectra were acquired on a 1.5 mM uniformly ^{13}C–^{15}N-

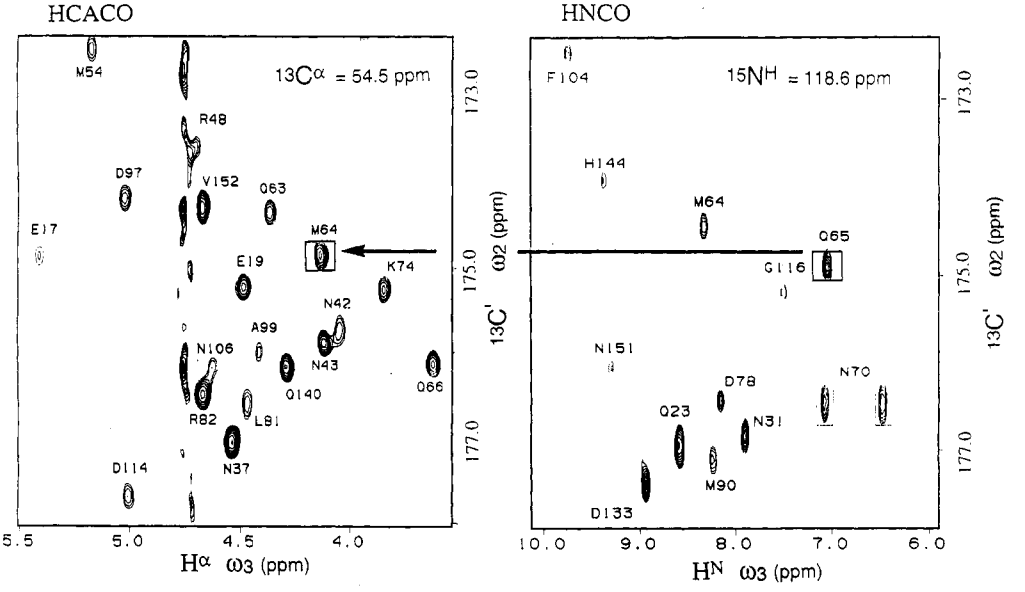

FIGURE 3: Representative cross-sections of the HCACO (A, left) and HNCO (B, right) spectra of ^{13}C–^{15}N-labeled eCyP. The HCACO cross plane is at a fixed ω_1 position corresponding to $^{13}C^{\alpha}$ nuclei with chemical shifts at or near 54.5 ppm. Cross peaks record the $^1H^{\alpha}(\omega_3)$ and $^{13}C'(\omega_2)$ chemical shifts of the indicated residues. The HNCO spectrum (right) is taken at a $^{15}N^H(\omega_2)$ frequency of 118.6 ppm and shows those residues whose amide nitrogens resonate at or near this frequency. Each cross peak correlates the $^1H^N(\omega_3)$ of residue i with the $^{13}C'$ of residue $i-1$. Cross peaks are labeled according to the sequence number of residue i. A line connects the correlations of Met64 (HCACO) and Gln65 (HNCO), demonstrating their sequential linkage.

Table I: Chemical Shifts for the Assigned Proton, Carbon-13, and Nitrogen-15 Backbone Resonances of the Periplasmic Cyclophilin Type *cis–trans* Peptidyl-Prolyl Isomerase from *Escherichia coli* (eCyP)

residue	$^1H^N$ [a]	^{15}NH [c]	$^1H^\alpha$ [a]	$^{13}C^\alpha$ [b]	$^{13}C'$ [b]	residue	$^1H^N$ [a]	^{15}NH [c]	$^1H^\alpha$ [a]	$^{13}C^\alpha$ [b]	$^{13}C'$ [b]	residue	$^1H^N$ [a]	^{15}NH [c]	$^1H^\alpha$ [a]	$^{13}C^\alpha$ [b]	$^{13}C'$ [b]
Ala1′			4.02	50.1	172.4	Gln56	9.12	130.0	5.43	52.0	173.2	Phe112	7.16	115.0	4.49	55.4	174.6
Ala1	*8.06	*12 7.1	4.41	50.5	176.3	Gly57	8.29	113.9	*3.03, *5.21	44.3	171.4	Leu113	7.27	124.2	4.61	52.9	174.3
Lys2	8.46	124.5	4.26	55.2	175.9	Gly58	7.47	106.0		45.1	172.3	Asp114	7.38	121.0	5.04	53.1	176.6
Gly3	8.51	114.3	*3.95	43.3	172.7	Gly59	9.82	109.0	3.21, 4.61	44.1	169.9	His115	8.65	123.3	4.01	55.9	174.1
Asp4	8.12	127.2	5.13	51.6	173.9	Phe60	9.68	124.6	5.22	55.4	175.5	Gly116	7.52	117.8	3.61, 4.21	43.4	
Pro5			4.62	61.4	175.0	Thr61	8.58	113.4	4.74	58.8	175.2	Gln117	8.22	122.4	4.06	56.2	175.7
His6	9.51	123.2	6.01	52.1	173.3	Glu62	9.51	122.7	3.98	57.7	175.6	Arg118	8.46	120.3	4.31	55.5	174.3
Val7	8.65	123.7	5.05	58.1	172.0	Gln63	7.56	120.1	4.36	54.0	173.3	Asp119	7.65	121.8	*4.75	52.1	173.4
Leu8	9.30	132.2	5.07	51.6	174.9	Met64	8.35	117.9	4.16	54.0	173.8	Phe120			4.07	59.2	175.9
Leu9	9.83	132.0	4.96	51.6	173.7	Gln65	7.08	118.9	4.56	52.6	174.1	Gly121	8.65	105.4	3.96	43.0	172.5
Thr10	9.13	127.1	4.82	60.7	173.6	Gln66	8.86	128.9	3.63	54.0	175.1	Tyr122	8.32	123.6	5.28	56.0	174.1
Thr11	7.97	120.8	6.14	57.8	175.6	Lys67	7.65	130.2	4.12	54.8	174.6	Ala123	9.40	130.8	4.21	51.3	174.0
Ser12	9.62	120.6	4.24	59.3	172.4	Lys68	8.56	129.6	4.54	52.9	173.4	Val124	9.65	132.3	4.32	60.6	174.7
Ala13	8.28	126.1	4.62	49.7	174.1	Pro69			4.81	60.8	174.8	Phe125	8.16	119.9	4.97	52.9	172.0
Gly14	7.37	109.9	3.80, 4.67	42.1	173.5	Asn70	8.51	121.4	4.93	50.8	171.3	Gly126	7.18	109.3	3.85, 4.0	44.8	170.4
Asn15	9.06	125.7	5.79	51.0	173.7	Pro71						Lys127	8.61	120.8	5.06	52.8	172.5
Ile16	8.99	123.6	4.60	59.1	172.6	Pro72			5.01	60.8	175.9	Val128	9.14	126.9	4.06	61.3	175.5
Glu17	9.19	132.2	5.39	52.9	173.8	Ile73	8.19	113.9	4.56	57.4	173.9	Val129	8.91	126.3	4.52	59.7	174.6
Leu18	9.54	130.0	5.11	51.1	174.5	Lys74	7.84	124.5	3.86	54.1	174.3	Lys130	7.69	124.9	4.56	55.4	174.4
Glu19	9.01	124.6	4.46	53.8	174.2	Asn75	8.49	125.9	4.41	51.9	175.8	Gly131	8.91	114.9		44.5	175.3
Leu20	8.73	132.5	4.76	52.3	172.3	Glu76	7.96	131.1	4.67	54.9	173.8	Met132	9.00	125.8	4.61	54.8	176.2
Asp21	8.16	125.3	4.58	50.8	173.3	Ala77	9.36	123.5	4.63	52.7	175.4	Asp133	8.96	118.6	4.39	54.5	177.5
Lys22	7.94	128.1	3.75	57.2	175.9	Asp78	8.17	117.4	3.60	51.3	174.3	Val134	7.30	127.9	3.44	64.2	176.1
Gln23	8.61	118.8	4.09	56.7	177.3	Asn79	8.16	121.8	4.38	52.0	174.9	Ala135	7.64	125.2	3.68	53.8	177.7
Lys24	7.67	118.4	4.41	54.5	176.0	Gly80	8.18	111.8	3.59, 4.23	43.8	173.6	Asp136	8.49	120.5	4.33	55.6	178.9
Ala25	8.12	127.9	4.89	48.3	171.0	Leu81	7.89	124.2	4.49	53.0	175.6	Lys137	7.91	126.6	3.88	58.5	178.9
Pro26			4.34	64.8	180.3	Arg82	8.08	125.2	4.70	53.7	175.4	Ile138	8.60	124.5	3.48	64.0	175.2
Val27	9.99	126.3	3.63	65.0	178.3	Asn83	*11.26	*129.8	4.68	52.8	175.4	Ser139	7.80	115.1	3.86	60.0	171.8
Ser28	9.74	123.9	3.96	60.1	176.7	Thr84	8.27	117.0	4.42	59.0	174.3	Gln140	7.03	120.6	4.31	54.0	175.2
Val29	9.29	126.3	3.51	67.0	175.0	Arg85	9.24	126.2	3.26	57.1	174.3	Val141	7.29	120.8	4.41	59.3	172.2
Gln30	7.69	121.9	3.86	57.0	175.7	Gly86	9.0	117.9	4.0, 4.51	43.6	172.1	Pro142			4.49	63.0	176.9
Asn31	7.93	119.1	4.12	55.1	173.7	Thr87	7.85	113.1	4.71	59.5	171.3	Thr143	8.43	115.6	5.13	58.0	172.7
Phe32	7.83	121.7	4.48	60.7	176.6	Ile88	7.20	121.1	5.11	55.6	169.4	His144	9.40	118.6	4.93	51.6	170.6
Val33	8.91	120.4	3.40	65.2	176.0	Ala89	8.54	132.9	5.49	48.4	176.0	Asp145	8.21	121.9	5.27	51.8	175.1
Asp34	8.39	125.0	4.40	56.0	179.4	Met90	8.26	118.7	5.61	50.8	176.6	Val146	8.55	125.5	3.98	59.7	173.7
Tyr35	7.50	124.1	3.94	60.8	177.1	Ala91	8.53	129.6	4.83	49.7	174.6	Gly147	8.77	120.7		43.0	
Val36	8.47	122.9	3.56	64.8	179.6	Arg92	8.03	115.6	*4.75	53.5	174.6	Pro148			4.36	61.5	174.3
Asn37	9.34	121.8	4.53	53.8	176.0	Thr93	*8.12	*114.8	4.66	59.2	172.3	Tyr149	8.11	126.3	4.46	56.2	173.3
Ser38	7.94	116.6	4.54	57.5	174.1	Ala94	8.00	123.8	4.01	53.9	177.5	Gln150	8.36	123.7	4.89	52.5	175.0
Gly39	7.93	113.7	3.96, 4.34	44.2	174.4	Asp95	8.23	119.6	4.56	52.4	176.7	Asn151	9.31	117.9	3.97	54.2	171.3
Phe40	8.11	124.8	3.76	60.2	175.3	Lys96			3.78	58.4	176.1	Val152	8.26	122.8	4.56	57.5	174.9
Tyr41	7.42	113.5	4.49	56.3	175.6	Asp97	8.57	126.0	5.04	53.1	173.2	Pro153			4.41	62.7	175.5
Asn42	7.38	125.7	4.06	53.0	174.6	Ser98	6.75	111.2	4.49	56.7	174.6	Ser154	8.77	125.4	3.47	59.5	172.9
Asn43	9.54	120.8	4.13	54.0	174.7	Ala99	8.88	133.0	4.41	52.7	175.0	Lys155	7.96	126.6	4.81	50.9	171.9
Thr44	7.86	111.4	5.00	60.2	172.7	Thr100	9.17	113.9	4.89	57.7	171.6	Pro156			4.33	62.0	175.3
Thr45	7.97	108.4	5.52	58.2	177.8	Ser101	8.80	116.5	4.37	56.1	175.0	Val157	9.61	129.8	4.02	60.6	173.2
Phe46	8.26	123.0	5.06	58.1	173.6	Gln102	8.21	125.7	4.88	55.7	173.0	Val158	8.29	129.8	4.16	60.3	175.4
His47	7.83	124.7	4.56	55.2	171.9	Phe103	7.99	121.4	6.04	52.6	171.4	Ile159	9.47	130.6	3.89	60.9	172.6
Arg48	6.97	126.3	4.72	53.8	172.6	Phe104	9.77	119.4	5.93	53.6	171.4	Leu160	8.84	134.6	4.03	55.7	177.1
Val49	8.82	125.0	4.82	58.0	171.7	Ile105	9.03	121.7	4.87	57.2	175.5	Ser161	7.72	110.9	4.48	55.5	170.3
Ile50	8.23	125.6	4.86	55.8	171.9	Asn106	8.74	129.3	4.63	53.6	175.3	Ala162	7.96	128.4	5.55	48.6	173.7
Pro51			4.06	61.7	176.5	Val107	8.13	121.1	4.57	59.1	171.9	Lys163	8.26	121.9	4.66	53.2	173.3
Gly52	9.29	112.6	3.66, 3.96	43.7	171.8	Ala108	7.75	129.4	4.49	48.8	171.7	Val164	9.03	128.7	4.49	61.1	175.1
Phe53	7.78	119.9	5.29	55.4	173.1	Asp109	8.31	120.0	4.61	52.8	173.4	Leu165	8.61	133.9	4.60	51.2	172.9
Met54	8.21	119.9	5.16	53.3	171.4	Asn110	8.29	132.7	4.93	49.6	173.3	Pro166					
Ile55	7.92	113.1	4.87	58.1	171.4	Ala111	7.96	127.9	4.21	53.1	177.5						

[a] Proton chemical shifts are referenced to TSP. [b] Carbon-13 chemical shifts are referenced to dioxane. [c] Nitrogen-15 chemical shifts are referenced to $NH_4{}^{15}NO_2$ in ^2H_2O (25 °C, 376.25 ppm). Residues marked with an * are tentatively assigned.

enriched eCyP sample. HCACO and HNCO spectra (Kay et al., 1990a) were acquired on a 700 μM sample of eCyP uniformly enriched with nitrogen-15 and 70% enriched with carbon-13.

A set of CT-HNCA and CT-HN(CO)CA spectra was used to link adjacent residues on the basis of their $^{13}C^\alpha$-chemical shifts. Figure 2 demonstrates how both spectra were used in conjunction to sequentially link Asp109 through His114. The CT-HNCA spectrum (top of Figure 2) provides intraresidue amide $^1H^N_{(i)}(\omega_3)$–$^{15}N_{(i)}(\omega_1)$ to $^{13}C^\alpha_{(i)}(\omega_2)$ correlations with a few sequential cross peaks to the preceding $^{13}C^\alpha_{(i-1)}(\omega_2)$ nucleus. The CT-HN(CO)CA spectrum (bottom of Figure 2) provides only sequential cross peaks ($^1H^N_{(i)}(\omega_3)$–$^{15}N_{(i)}(\omega_1)$ to $^{13}C^\alpha_{(i-1)}(\omega_2)$) complementing the CT-HNCA spectrum. Sequential cross peaks are enclosed by boxes in Figure 2. On the basis of secondary structure alignments, we predict that Phe112 and Leu113 are involved in cyclosporin binding (Neri et al., 1991; Spitzfaden et al., 1992; Fesik et al., 1992), while Leu113 may also be important in binding the tetrapeptide substrate AC-A-A-P-A-AMC (Kallen et al., 1991; Kallen & Walkinshaw, 1992).

Sequential linkage of adjacent residues was also accomplished via the backbone carbonyl ($^{13}C'$) nuclei. Figure 3 shows representative spectra from both HNCO and HCACO spectra of eCyP. The HCACO spectrum exhibits correlations between the $^1H^\alpha$, $^{13}C^\alpha$, and $^{13}C'$ nuclei. Figure 3A shows a cross plane of this spectrum taken at a fixed $^{13}C^\alpha(\omega_1)$ chemical shift. Cross peaks correlate the $^1H^\alpha$ and $^{13}C'$ nuclei of the indicated residues. The HCACO spectrum in conjunction with the CT-HNCA and TOCSY-HMQC (and/or CT-HN-

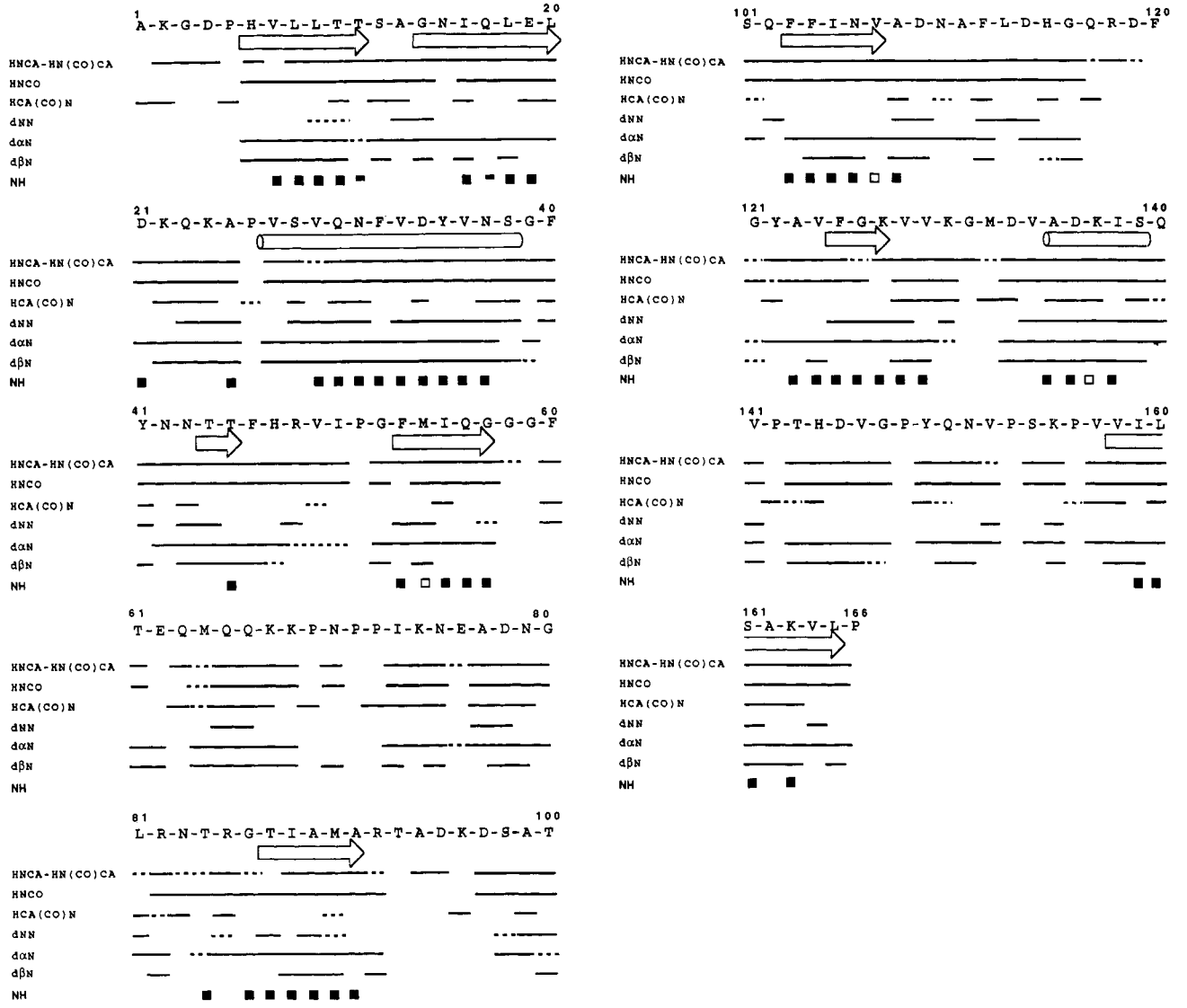

FIGURE 4: Summary of the sequential scalar and distance connectivities observed in the 3D triple- and double-resonance spectra of eCyP. The first three rows correspond to scalar connectivities observed in triple-resonance spectra. Rows marked HNCA–HN(CO)CA are observed $C_{\alpha i-1}$–N_i and H_i^N connectivities, HNCO are observed CO_{i-1}–N_i and H_i^N connectivities, and HCA(CO)N are observed $H_{\alpha i}$ and $C_{\alpha i}$–N_{i+1} connectivities. Rows 4–6 correspond to distance connectivities observed in ^1H–^{15}N NOESY-HMQC spectrum. Lines in the d_{NN} row correspond to NOEs between the amide protons of residues i and $i-1$. NOEs between the amide proton of residue i and the α- and β-protons of residue $i-1$ are marked on rows $d_{\alpha N}$ and $d_{\beta N}$, respectively. Dashed lines correspond to connectivities that are ambiguous due to resonance overlap or correlations that are very weak in intensity. Closed boxes in row 7 correspond to slowly exchanging amide protons as judged by protection from exchange after 1 day. Closed boxes cut in half have significantly reduced intensity after 1 day and therefore exhibit intermediate exchange behavior. Open boxes correspond to amides with ambiguous exchange behavior due to resonance overlap. Arrows and cylinders directly below the sequences indicate β-sheet and α-helical secondary structure, respectively.

(CA)HA) spectra allows complete correlation of all backbone nuclei in a residue. The HNCO experiment provides complementary sequential information. Figure 3B is a representative plot of the HNCO spectrum taken at a fixed (ω_1) chemical shift of the nitrogen-15 nucleus. Each cross peak correlates the $^1H^N$ of the indicated residue with the preceding $^{13}C'$ nucleus. The sequential connectivity of Gln65 to Met64 is indicated by an arrow at the appropriate $^{13}C'$ chemical shift.

Analysis of double- and triple-resonance data resulted in the complete or partial backbone assignment of 165 of the 167 residues in eCyP. Resonance assignments are listed in Table I for residues 23–190 of eCyP (sequence numbers as listed by Liu and Walsh (1990)). Completion of the backbone assignments revealed the presence of an extra alanine residue at the N-terminus of eCyP. In order to maintain consistency with our preestablished numbering system, this residue is denoted Ala1′ and corresponds to position 23 of procyclphilin. Residues labeled 1–166 correspond to residues 24–190 of procyclophilin. Of 155 possible amide resonances ($^{15}N^N$–$^1H^N$ correlations) (167 total residues, 11 prolines, N-terminus), all were assigned except for three. The unassigned $^{15}N^N$–$^1H^N$ correlations belong to Thr93, Lys96, and Phe120. Correlations for these three residues were not found in any amide-detected triple-resonance experiment. However, the $^1H^\alpha$, $^{13}C^\alpha$, and $^{13}C'$ chemical shifts of these residues were determined by observation of sequential connectivities in the HNCO and HN(CO)CA spectra. For each of the three residues, the process of elimination left only one correlation in the HCA(CO)N and HCACO spectra that could satisfy the assignment at any of these positions. For example, there are three residues that have the proper $^{13}C^\alpha$ chemical shift (Thr61, Thr84, and Lys137) to fit into the position of Lys96. These correlations, however, possess either $^1H^\alpha$ chemical shifts and/or NOE patterns that define their position elsewhere, excluding placement at position 96 in the sequence (see Figure

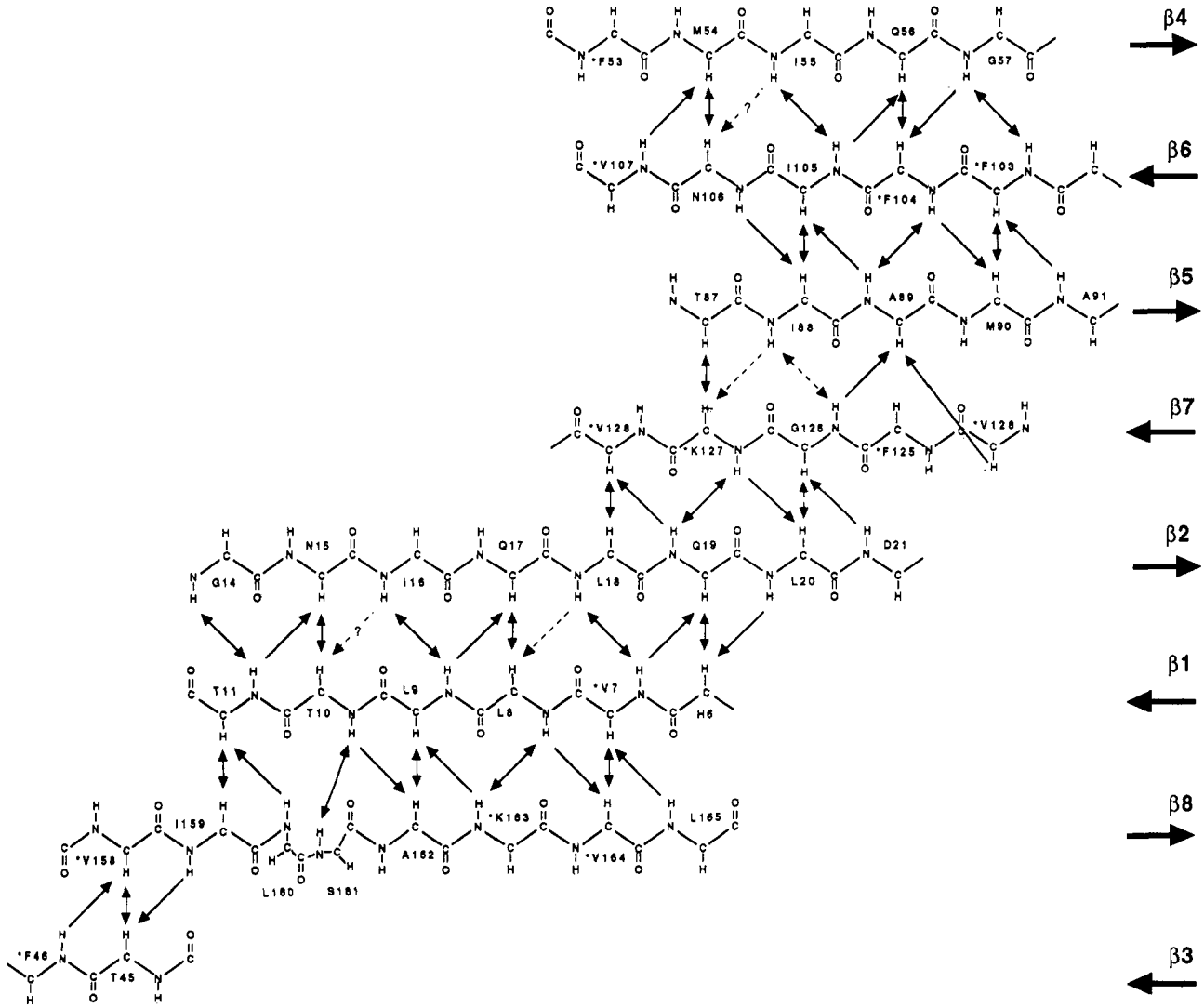

FIGURE 5: β-Sheet secondary structure of the cyclophilin type peptidyl-prolyl isomerase from *E. coli* (eCyP). The eight strands of the β-sheet are labeled (1–8). Arrows indicate observed NOE connectivities. The side chains of residues marked with * were identified by selective enrichment with nitrogen-15. Dashed arrows indicate tentatively assigned NOEs because of resonance overlap. Arrows with "?" in the center indicate NOEs that are expected on the basis of anti-parallel secondary structure, but are nonetheless absent. All $d_{\alpha\alpha}$ NOEs (double-headed arrows) were unambiguously identified in ^{13}C-dispersed NOESY spectra.

4). Residues encompassing Thr93, Lys96, and Phe120 undergo rapid exchange with the solvent, exhibiting only a few cross peaks of weak intensity in the HMQC-NOESY spectrum, which employed presaturation to eliminate the H_2O signal. Preliminary solution structure calculations of eCyP based on >600 NMR derived distance constraints (R. T. Clubb, S. B. Ferguson, C. T. Walsh, and G. Wagner, manuscript in preparation) indicate that these three residues participate in solvent-accessible loops. Two of the three unassigned residues (Lys96 and Phe120) fail to appear in HSQC spectra of selectively enriched samples of eCyP ([^{15}N]-lysine and [^{15}N]phenylalanine). This may be due to chemical shift degeneracy (either with another amide of similar side-chain type or with the H_2O signal) or extreme broadening of the ^1H–^{15}N correlation. In the case of Phe120, the selectively labeled sample was quite dilute (~200 μM), further hindering assignment.

Carbonyl chemical shifts for all glycine residues were obtained from the HNCO spectrum. Glycine $^1H^{\alpha}$–$^{13}C^{\alpha}$–$^{13}C'$ correlations did not appear in the HCACO spectrum of eCyP. This can readily be explained by the choice of delays used in the $^1H^{\alpha}$–$^{13}C^{\alpha}$ INEPT portion of the HCACO pulse sequence. A value of 1.5 ms was used to approximate $^1/_4J_{^{13}C^{\alpha}-^1H^{\alpha}}$, which is ideal for methine groups but too long for methylenes (a value of ca. 750 μs should be used for glycine observation). The backbone nuclei of Pro71 and Pro166 have not been unambiguously assigned since these residues are not followed by amide-containing residues. There are two correlations left in the HCACO spectrum that could be fit into either of these positions. Neither of these $^1H^{\alpha}$–$^{13}C^{\alpha}$ correlations possesses a $^1H^{\alpha}_{(i)}$–$^{13}C^{\alpha}_{(i)}$–$^{15}N^{H}_{(i+1)}$ cross peak in the HCACON spectrum, and they both therefore remain unassigned.

Double- and triple-resonance NMR techniques provided several avenues to sequence and specifically assign adjacent residues. A summary of the sequential connectivities observed in eCyP is shown in Figure 4. Lines drawn below the sequence of eCyP indicate that a sequential connectivity was observed, while dashed lines below each residue indicate that either resonance overlap or weak intensities resulted in ambiguous linkage. The first three rows of lines in Figure 4 summarize information obtained from triple-resonance spectra of eCyP. Rows 4–6 summarize information obtained from the ^1H–^{15}N NOESY-HMQC spectrum. Observed secondary structural elements (arrows for β-sheets and cylinders for α-helices) are shown directly below the sequences. Assigned secondary structural elements are clearly supported by the observed NOE constraints (rows 4–6). For example, residues involved in helical secondary structure exhibit abundant d_{NN} connectiv-

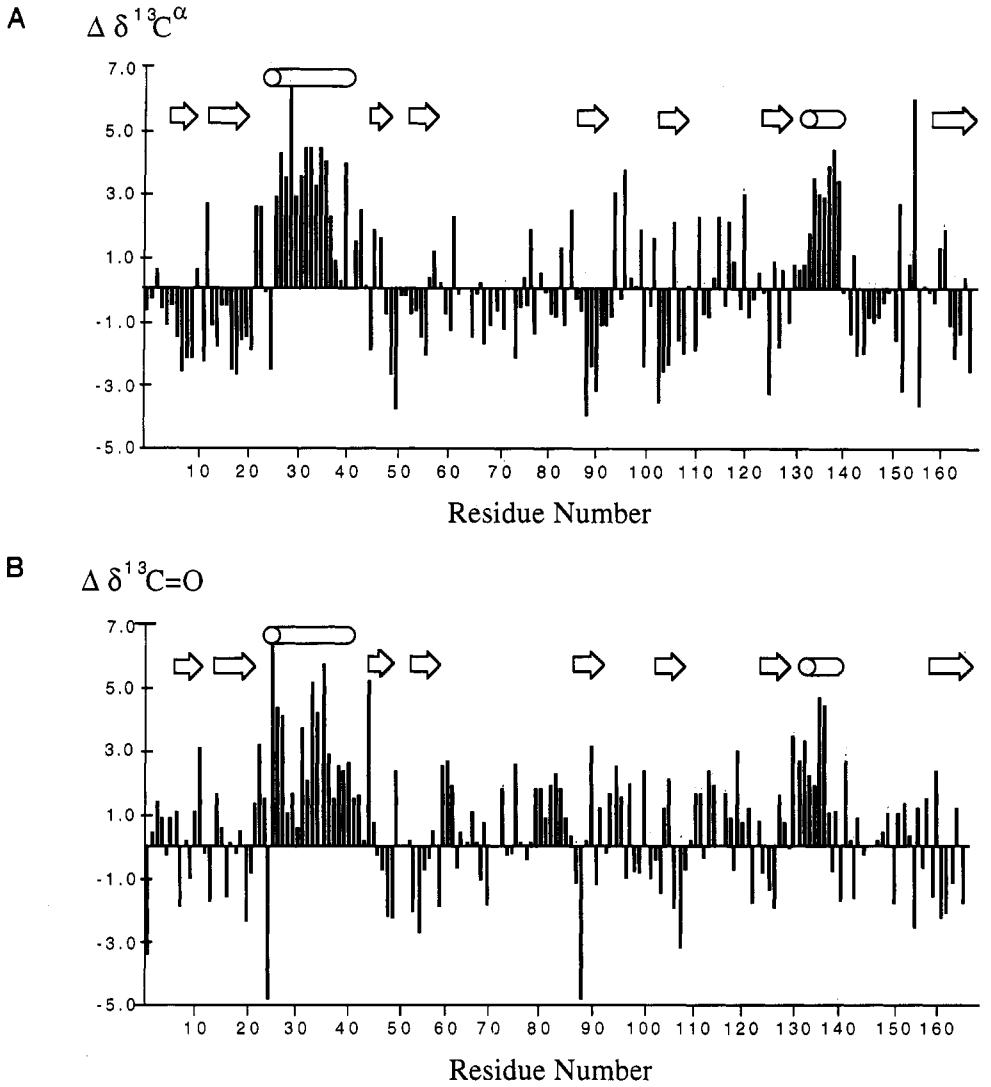

FIGURE 6: Carbon chemical shift comparison of backbone eCyP nuclei with those of an unstructured peptide. Part A is a plot of eCyP α-carbon chemical shifts minus random coil values ($\Delta\delta^{13}C^{\alpha}$) versus sequence number. Part B shows a plot of carbonyl chemical shifts minus random coil values ($\Delta\delta^{13}C'$) versus sequence number. Arrows and cylinders represent β-sheet and helical secondary structure, respectively. Random coil carbon chemical shifts for each amino acid (Richarz & Wüthrich, 1978) were subtracted from the values listed in Table I.

ities. In general, residues participating in well-defined secondary structure also exhibit retarded amide proton exchange with the solvent (denoted by square symbols in row 7).

Close inspection of Figure 4 reveals that there are several regions in eCyP where sequence-specific assignment is based on only a few sequential linkages. In particular, several regions in eCyP exhibited few NOEs and therefore proved difficult to assign unambiguously by utilizing conformation-dependent constraints alone. These regions include Ala1′–Asp4, Val49–Ile50, Gly57–Gly59, Glu62–Gln63, Glu76, Asn83, Arg92–Asp97, Gln117–Phe120, and Gly131. All of these regions appear to be solvent-accessible and undergo rapid amide exchange. When a purge pulse (Messerli et al., 1989) is used instead of presaturation, as was the case in the HNCA and HN(CO)CA experiments, this problem can be overcome. Purge pulse suppression of the H_2O resonance facilitated the observation of all residues except the aforementioned Thr93, Lys96, and Phe120. One of these regions exhibits very narrow line widths (Ala1′–Asp4) and is assumed to undergo rapid motion. Interpretation of ^1H–^{15}N NOESY-HMQC spectra was further hindered by the chemical heterogeneity of the ^{15}N-labeled sample. Resonances corresponding to His6–Leu9, Ile16–Leu23, and Val129–Asp136 are duplicated in the ^1H–^{15}N NOESY-HMQC spectrum. The source of this heterogeneity is unknown but most likely results from chemical modification of eCyP (e.g., deamidation), since other labeled samples appear homogeneous.

The CT-HNCA, CT-HN(CO)CA, HNCO, and HCACO experiments were clearly the most useful in obtaining the sequential assignments of eCyP (see Figure 4). In particular, if presaturation was avoided in the HNCA and HN(CO)CA experiments, this facilitated the assignment of several regions. The HCA(CO)N, while providing sequential connectivities, was less sensitive and therefore less useful. The HN(CA)HA experiment, while clearly less sensitive than the HNCA, provided crucial intraresidue ^{15}N–$^1H^{\alpha}$, and $^1H^N$ information, facilitating the analysis of both HCACO and NOESY-HMQC spectra.

DISCUSSION

During the process of sequence-specific resonance assignment, concurrent analysis of the NOESY-HMQC spectrum yielded information about the secondary structure and aided in further assignments. Tertiary NOEs revealed that eCyP consists of an eight-stranded anti-parallel β-sheet and two helices. The overall topology of this β-sheet is shown in Figure 5. The strands of the sheet are labeled from 1 to 8,

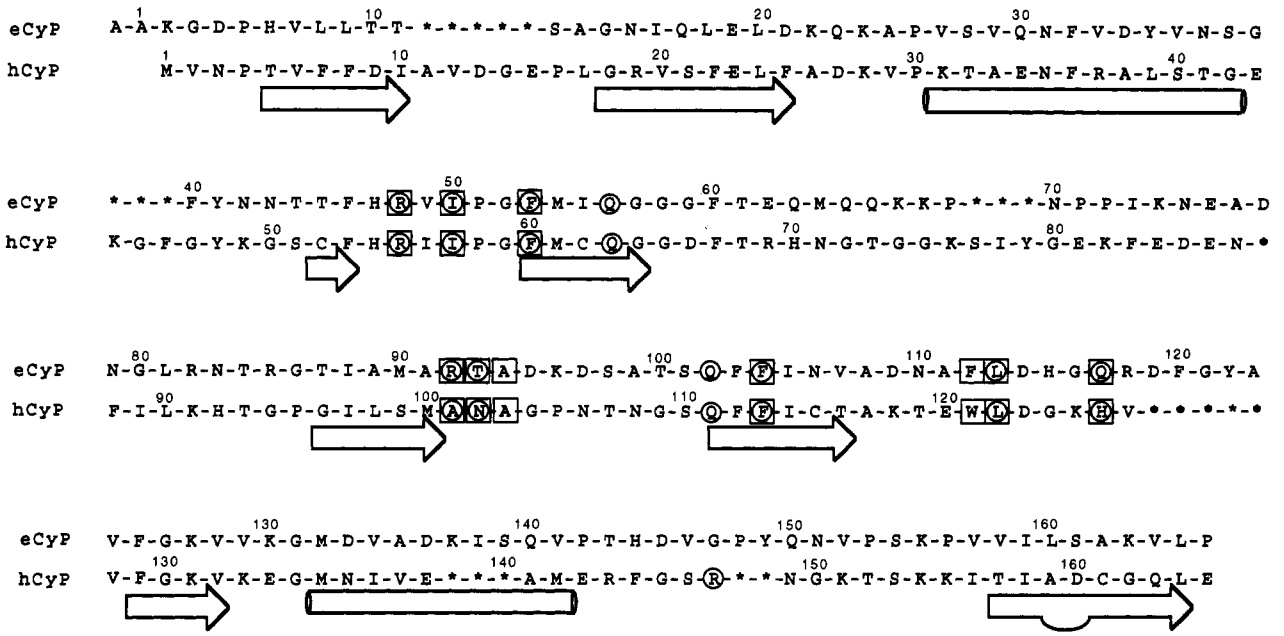

FIGURE 7: Alignment of eCyP and hCyP amino acid sequences based on secondary structure. The top sequence corresponds to eCyP; the lower sequence is hCyP. Arrows and cylinders below both sequences indicate β-sheet and helical secondary structure, respectively. Residues in hCyP enclosed in boxes were identified in NMR studies to possess protons within 5 Å of CsA (Neri et al., 1991; Spitzfaden et al., 1992; Fesik et al., 1992). Homologous residues in eCyP are indicated by enclosure in boxes. Residues of hCyP enclosed by circles have heavy atoms within 3.5 Å of the tetrapeptide substrate AC-A-A-P-A-AMC (Kallen et al., 1991; Kallen & Walkinshaw, 1992). Homologous residues in eCyP are similarly enclosed by circles. No residue in eCyP homologous to Arg148 of hCyP has been identified.

corresponding to increasing residue number. Strand 1 consists of residues His6–Thr11, strand 2 Gly14–Asp21, strand 3 Thr45–Phe46, strand 4 Phe53–Gly57, strand 5 Thr87–Ala91, strand 6 Phe103–Val107, strand 7 Phe125–Val128, and strand 8 Val158–Leu165. The helices (not shown in Figure 5) consist of residues Val27–Ser38 and Asp133–Val141.

The secondary structure of eCyP is manifested in the chemical shifts of its backbone nuclei. In order to remove primary sequence contributions, the carbon chemical shifts of amino acids in unstructured peptides were subtracted from those of eCyP (Richarz & Wüthrich, 1978). As observed in other proteins (Ikura et al., 1990; Spera & Bax, 1991; Wishart et al., 1991; Grzesiek et al., 1992b; Lee et al., 1992), a plot of these differences versus the sequence of eCyP reveals a strong correlation with secondary structure. Figure 6A shows a plot of $^{13}C^{\alpha}$ chemical shift differences versus sequence number. The helices (Val27–Ser38 and Asp133–Val141) in general exhibit downfield shifts from unstructured peptides, while the eight β-sheet strands exhibit a less consistent upfield shift from random coil values. Figure 6B illustrates the effects of secondary structure on backbone carbonyl chemical shifts in eCyP. Similar to the $^{13}C^{\alpha}$ chemical shifts, the carbonyl nuclei exhibit a downfield shift when involved in helices and turns and a less consistent upfield shift when involved in β-sheets. Larger variations in the backbone ϕ,ψ dihedral angles of β-sheet-participating residues readily explain the less consistent upfield shifts of their $^{13}C^{\alpha}$ and $^{13}C'$ nuclei (Spera & Bax, 1991). Interestingly, a comparison of Figure 6A,B reveals that the $^{13}C^{\alpha}$ chemical shifts exhibit significantly more consistent correlations with sheet type structures than do the $^{13}C'$ shifts of eCyP.

The overall secondary structure topology of eCyP is similar to that of human cyclophilin, consistent with ca. 35% sequence homology between the two proteins. A comparison of the secondary structural elements of the two proteins facilitates an alignment of their sequences (shown in Figure 7). There are two major differences between the two proteins: (1) In the human cyclophilin, there is a β-bulge in strand 2 consisting of residues Leu17 and Gly18 (hCyP numbering). In eCyP, however, there is no evidence for a β-bulge; instead, the bulge is replaced by a turn connecting strands 1 and 2. (2) In contrast to hCyP, no evidence has been observed for backbone hydrogen bonding between strands 3 and 4 in eCyP. However, preliminary structure calculations do place strands 3 and 4 in close proximity indicating that eCyP does possess a barrel type solution structure.

If we assume that the overall global folds of eCyP and hCyP are similar (supported by our observations), alignment of the two sequences provides information about the relative importance of eCyP residues in CsA binding and PPIase activity. Figure 7 shows alignment of the amino acid sequences of hCyP and eCyP based on secondary structure. Human cyclophilin residues enclosed in boxes have protons within 5 Å of bound CsA (Ke et al., 1991; Kallen et al., 1991; Fesik et al. 1992). Alignment of eCyP and hCyP indicates that these 10 residues in hCyP correspond to Arg48, Ile50, Phe53, Gln56, Arg92, Thr93, Ala94, Phe112, Leu113, and Gln117 in eCyP (residues also enclosed in boxes in eCyP). Of these 10 residues, six are conserved between the human and *E. coli* proteins. The four differences correspond to residues Arg92, Thr93, Phe112, and Gln117 of eCyP. Since their global folds are similar, the large differences in the affinities of these proteins for CsA (hCyP, IC_{50} = 6 nM; eCyP, IC_{50} = 3000 nM) (Handschumacher et al., 1984; Harding et al., 1986; Liu et al., 1990) can be attributed to these residues. Mutagenesis of Phe112 to Trp112 in eCyP resulted in a 23-fold increase in affinity for the drug CsA, supporting our secondary structure alignment (Liu et al., 1991a). Residues that have heavy atoms within 3.5 Å of the tetrapeptide substrate AC-A-A-P-A-AMC used in the crystal structure analysis of hCyP are enclosed in circles (Kallen et al., 1991; Kallen & Walkinshaw, 1992). Of these 11 residues, 10 could be unambiguously aligned with eCyP (residues also enclosed in circles in eCyP); there is no obvious homolog for the Arg148 of hCyP. Of the 10 aligned residues, seven are conserved between eCyP and hCyP. The differences correspond to Arg92, Thr93, and Gln117.

CONCLUSION

We have assigned nearly all $^{1}H^{\alpha}$, $^{1}H^{N}$, $^{15}N^{H}$, $^{13}C^{\alpha}$, and $^{13}C'$ backbone nuclei in the periplasmic cyclophilin type peptidyl-prolyl isomerase from *E. coli*. Assignments were obtained using a series of 3D double- and triple-resonance NMR experiments. Backbone assignments facilitated the identification of tertiary NOEs in the ^{1}H–^{15}N NOESY-HMQC spectrum, allowing the secondary structure of the protein to be determined. The overall fold appears to be similar to that of human cyclophilin, an eight-stranded anti-parallel β-sheet barrel with two helices. A secondary structure alignment with human cyclophilin implicates 10 residues in eCyP that should be important for CsA binding. Four of the 10 residues are not conserved from humans to *E. coli* and may help to explain the reduced affinity of eCyP for the drug CsA relative to hCyP. Alignment also reveals a high degree of sequence conservation of residues thought to be important for PPIase activity. Of the 11 residues proximal to the tetrapeptide substrate, at least seven are conserved in eCyP.

Assignments laid the foundation for obtaining extensive side-chain assignments with HCCH-COSY (Kay et al., 1990b; Bax et al., 1990a) and HCCH-TOCSY (Fesik et al., 1990; Bax et al., 1990b) experiments. These assignments will be invaluable in the interpretation of 4D $^{15}N/^{13}C$- and 3D and 4D $^{13}C/^{13}C$-edited NOESY spectra. The structural information thus obtained will aid in understanding the mechanism of peptidyl-prolyl isomerization and the structural basis of binding of the immunosuppressant drug CsA. Characterization of the surface structure of eCyP will identify the conserved features between hCyP and eCyP that are responsible for interaction and inhibition of calcineurin.

ACKNOWLEDGMENT

We thank Drs. Sven Hyberts, Jonathan P. Lee, and N. R. Nirmala and Mr. Jeff W. Peng for useful discussions. We also thank Ms. Zhiyuh Chang for assistance in preparing the amino acid specific ^{15}N-enriched samples.

REFERENCES

Bax, A., & Davis, D. G. (1985) *J. Magn. Reson. 65*, 355–360.
Bax, A., & Ikura, M. (1991) *J. Biomol. NMR 1*, 99–104.
Bax, A., Clore, G. M., Driscoll, P. C., Gronenborn, A. M., Ikura, M., & Kay, L. E. (1990a) *J. Magn. Reson. 87*, 620–627.
Bax, A., Clore, G. M., & Gronenborn, A. M. (1990b) *J. Magn. Reson. 88*, 425–431.
Billeter, M., Braun, W., & Wüthrich, K. (1982) *J. Mol. Biol. 155*, 320–346.
Bodenhausen, G., & Ruben, D. L. (1980) *Chem. Phys. Lett. 69*, 185–188.
Braunschweiler, L., & Ernst, R. R. (1983) *J. Magn. Reson. 53*, 521–528.
Brown, S. C., Weber, P. L., & Mueller, L. (1988) *J. Magn. Reson. 77*, 166–169.
Clubb, R. T., Thanabal, V., Osborne, C., & Wagner, G. (1991) *Biochemistry 30*, 7718–7730.
Clubb, R. T., Thanabal, V., & Wagner, G. (1992) *J. Biomol. NMR 2*, 203–210.
Driscoll, P. C., Clore, G. M., Marion, D., Wingfield, P. T., & Gronenborn, A. M. (1990) *Biochemistry 29*, 3542–3556.
Dubs, A., Wagner, G., & Wüthrich, K. (1979) *Biochem. Biophys. Acta 577*, 177–194.
Fairbrother, W. J., Cavanagh, J., Dyson, H. J., Palmer, A. G., Sutrina, S. L., Reizer, J., Saier, M. H., & Wright, P. E. (1991) *Biochemistry 30*, 6896–6907.
Fesik, S., & Zuiderweg, E. R. P. (1988) *J. Magn. Reson. 78*, 588–593.
Fesik, S. W., Eaton, H. L., Olejniczak, E. T., Zuiderweg, E. R. P., McIntosh, L. P., & Dahlquist, F. W. (1990) *J. Am. Chem. Soc. 112*, 886–888.
Fesik, S. W., Gampe, R. T., Jr., Eaton, H. L., Gemmecker, G., Olejniczak, E. T., Neri, P., Holzman, T. F., Egan, D. A., Edalji, R., Simmer, R., Helfrich, R., Hochlowski, J., & Jackson, M. (1991) *Biochemistry 30*, 6574–6583.
Fesik, S. W., Neri, P., Meadows, R., Olejniczak, E. T., & Gemmecker, G. (1992) *J. Am. Chem. Soc. 114*, 3165–3166.
Fischer, G., Wittmann-Liebold, B., Lang, K., Kiefhaber, T., & Schmid, F. X. (1989) *Nature 337*, 476–478.
Grzesiek, S., & Bax, A. (1992) *J. Magn. Reson. 96*, 432–440.
Grzesiek, S., Dobeli, H., Gentz, R., Garotta, G., Labhardt, A. M., & Bax, A. (1992) *Biochemistry 31*, 8180–8190.
Handschumacher, R. E., Harding, M. W., Rice, J., Drugge, R. J., & Speicher, D. W. (1984) *Science 226*, 544–547.
Harding, M. W., Handschumacher, R. E., & Speicher, D. W. (1986) *J. Biol. Chem. 261*, 8547–8555.
Harding, M. W., Galat, A., Uehling, D. E., & Schreiber, S. L. (1989) *Nature 341*, 758–760.
Hayano, T., Takahashi, N., Kato, S., Maki, N., & Suzuki, M. (1991) *Biochemistry 30*, 3041–3048.
Ikura, M., Kay, L. E., & Bax, A. (1990) *Biochemistry 29*, 4659–4667.
Ikura, M., Spera, S., Barbato, G., Kay, L. E., Krinks, M., & Bax, A. (1991) *Biochemistry 30*, 9216–9228.
Jeener, J., Meier, B. H., Bachmann, P., & Ernst, R. R. (1979) *J. Chem. Phys. 71*, 4546–4553.
Kallen, J., & Walkinshaw, M. D. (1992) *FEBS 300*, 286–290.
Kallen, J., Spitzfaden, C., Zurini, M. G. M., Wider, G., Widmer, H., Wüthrich, K., & Walkinshaw, M. D. (1991) *Nature 353*, 276–279.
Kay, L. E., Ikura, M., Tschudin, R., & Bax, A. (1990a) *J. Magn. Reson. 89*, 496–514.
Kay, L. E., Ikura, M., & Bax, A. (1990b) *J. Am. Chem. Soc. 112*, 888–889.
Kay, L. E., Wittekind, M., McCoy, M. A., Friedrichs, M. S., & Mueller, L. (1992) *J. Magn. Reson. 98*, 443–450.
Ke, H., Zydowsky, L. D., Liu, J., & Walsh, C. T. (1991) *Proc. Natl. Acad. Sci. U.S.A. 88*, 9483–9487.
Kumar, R. M., Ernst, R. R., & Wüthrich, K. (1980) *Biochem. Biophys. Res. Commun. 95*, 1–6.
Lee, M. S., Palmer, A. G., & Wright, P. E. (1992) *J. Biomol. NMR 2*, 307–322.
Liu, J., & Walsh, C. T. (1990) *Proc. Natl. Acad. Sci. U.S.A. 87*, 4028–4032.
Liu, J., Chen, C. M., & Walsh, C. T. (1991a) *Biochemistry 30*, 2306–2310.
Liu, J., Farmer, J. D., Lane, W. S., Friedman, J., Weissman, I., & Schreiber, S. L. (1991b) *Cell 66*, 807–815.
Marion, D., & Wüthrich, K. (1983) *Biochem. Biophys. Res. Commun. 113*, 967–974.
Marion, D., Driscoll, P. C., Kay, L. E., Wingfield, P. T., Bax, A., Gronenborn, A., & Clore, G. M. (1989a) *Biochemistry 28*, 6150–6156.
Marion, D., Ikura, M., Tschudin, R., & Bax, A. (1989b) *J. Magn. Reson. 85*, 393–399.
McIntosh, L. P., Wand, A. J., Lowry, D. F., Redfield, A. G., & Dahlquist, F. W. (1990) *Biochemistry 29*, 6341–6362.
Messerli, B. A., Wider, G., Otting, G., Weber, C., & Wüthrich, K. (1989) *J. Magn. Reson. 85*, 608–613.
Morris, G. A., & Freeman, R. (1979) *J. Am. Chem. Soc. 101*, 760–762.
Muchmore, D. C., McIntosh, L. P., Russell, C. B., Anderson, D. E., & Dahlquist, F. (1989) *Methods Enzymol. 177*, 44–73.
Neri, P., Meadows, R., Gemmecker, G., Olejniczak, E., Nettesheim, D., Logan, T., Simmer, R., Helfrich, R., Holzman, T., Severin, J., & Fesik, S. (1991) *FEBS 294*, 81–88.
Ondeck, B., Hardy, R. W., Baker, E. K., Stamnes, M. A., Shieh, B.-H., & Zuker, C. S. (1992) *J. Biol. Chem. 267*, 16460–16466.

Piantini, U., Sørensen, O. W., Bodenhausen, G., Wagner, G., Ernst, R. R., & Wüthrich, K. (1982) *J. Am. Chem. Soc. 104*, 6800–6801.
Powers, R., Gronenborn, A. M., Clore, G. M., & Bax, A. (1991) *J. Magn. Reson. 94*, 209–213.
Rance, M., Sørensen, O. W., Bodenhausen, G., Wagner, G., Ernst, R. R., & Wüthrich, K. (1984) *Biophys. Biochem. Res. Commun. 117*, 479–485.
Richarz, R., & Wüthrich, K. (1978) *Biopolymers 17*, 2133–2141.
Siekierka, J. L., Hung, S. H. Y., Poe, M., Lin, C. S., & Sigal, N. H. (1989) *Nature 341*, 755–757.
Shaka, A. J., & Freeman, R. (1983) *J. Magn. Reson. 51*, 169–173.
Shaka, A. J., Keeler, J., Frenkiel, T., & Freeman, R. (1983) *J. Magn. Reson. 52*, 335–338.
Shaka, A. J., Lee, C. J., & Pines, A. (1988) *J. Magn. Reson. 77*, 274–293.
Spera, S., & Bax, A. (1991) *J. Am. Chem. Soc. 113*, 5490–5492.
Spitzfaden, C., Weber, H., Braun, W., Kallen, J., Wider, G., Widmer, H., Walkinshaw, M. D., & Wüthrich, K., (1992) *FEBS 300*, 291–300.
Stockman, B. J., Nirmala, N. R., Wagner, G., Delcamp, T. J., DeYarman, M. T., & Freisheim, J. H. (1992) *Biochemistry 31*, 218–228.
Takahashi, N., Hayano, T., & Suzuki, M. (1989) *Nature 337*, 473–475.
Weber, C., Wider, G., von Freyberg, B., Traber, R., Braun, W., Widmer, H., & Wüthrich, K. (1991) *Biochemistry 30*, 6563–6574.
Wishart, D. S., Sykes, B. D., & Richards, F. M. (1991) *J. Mol. Biol. 222*, 311–333.
Wüthrich, K. (1986) *NMR of Proteins and Nucleic Acids*, John Wiley & Sons, New York.
Wüthrich, K., Billiter, M., & Braun, W. (1984) *J. Mol. Biol. 180*, 715–740.
Wüthrich, K., Spitzfaden, C., Memmert, K., Widmer, H., & Wider, G. (1991) *FEBS 285*, 237–247.
Zuiderweg, E. R. P., & Fesik, S. W. (1989) *Biochemistry 28*, 2387–2391.